

# Reconciling STEM and X-ray Scattering Data from a Poly(styrene-*ran*-methacrylic acid) Ionomer: Ionic Aggregate Size

Nicholas M. Benetatos, Paul A. Heiney,<sup>†</sup> and Karen I. Winey\*

Department of Materials Science and Engineering,  
Department of Physics and Astronomy, University of  
Pennsylvania, Philadelphia, Pennsylvania 19104-6272

Received April 21, 2006

Revised Manuscript Received May 26, 2006

**Introduction.** Because of their extraordinary chemical and physical properties, ionomers have found wide-ranging applications including chemically resistant thermoplastics, coatings, and selectively permeable ion-transport membranes.<sup>1</sup> The unique properties of ionomers result directly from the self-assembly of ionic functional groups and counterions into nanoscale ionic aggregates. These transient physical cross-links strengthen the materials without eliminating their ability to be processed as thermoplastics. Despite numerous studies employing a multitude of experimental methods, the processing-structure-property relationships of ionomers are not comprehensively understood. Establishing the morphology of the ionic aggregates as a function of various chemical, physical, and processing parameters is critical to continuing the development of this important class of materials.

Small-angle X-ray scattering (SAXS) methods provide indirect experimental evidence for the existence of ionic aggregates and are widely employed in structural studies of ionomers.<sup>1</sup> SAXS data from ionomers typically exhibit a broad, isotropic scattering peak between 0.5 and 5 nm<sup>-1</sup>, although the origin and the interpretation of this peak remains a topic of some controversy. While several structural models have been suggested,<sup>2–4</sup> the most prevalent is that proposed by Yarusso and Cooper.<sup>5</sup> This model attributes the “ionomer” SAXS peak to interparticle interference between spherical, monodisperse, electron-rich scatterers arranged with liquidlike order in a matrix of lower electron density. The spatial correlation of the scatterers is determined both by the radius of the ion-rich region ( $R_1$ ) and by the radius of an excluded volume region surrounding each aggregate that limits the extent to which the ionic aggregates can pack together in space ( $R_{CA}$ ). When the two radii are equal, the Yarusso–Cooper model reduces to the hard-sphere interference model derived by Fournet.<sup>6</sup> A later version of the Yarusso–Cooper model incorporates the Percus–Yevick total correlation function<sup>7</sup> rather than the Fournet interference model; however, Kinning and Thomas found that both models can readily fit scattering data that exhibit only a single broad peak, as is typical for ionomers.<sup>8</sup> The Yarusso–Cooper model has been used to interpret a wide array of scattering data and has shown that the size of the ionic aggregates can vary significantly as a function of main chain characteristics and acid type but is relatively unaffected by the choice of neutralizing counterion.<sup>9</sup>

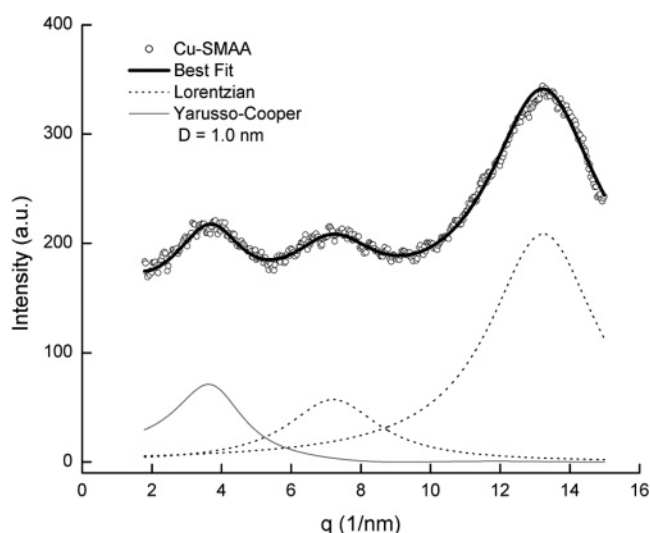


**Figure 1.** Scattered intensity as a function of scattering vector,  $q$ , for Cu-SMAA along with the best-fit model (solid). Our empirical model includes the Yarusso–Cooper model for interparticle scattering from spherical ionic aggregates (gray), two Lorentzian functions (dotted), and an additive constant.

The application of high-angle annular dark-field scanning transmission electron microscopy (HAADF-STEM) to the study of ionomer morphology has enabled direct, model-independent visualization of the ionic aggregates in thin specimens sectioned from bulk ionomers.<sup>10,11</sup> Recently, direct imaging methods have revealed a variety of morphologies as a function of copolymer type, counterion, and processing history that include inhomogeneous spatial distributions and nanoscale features of unexpected shape.<sup>12–15</sup> These findings are inconsistent with the assumptions of the Yarusso–Cooper model, although few studies exist in which the same ionomer is studied by both STEM and X-ray scattering.

We have recently shown that HAADF-STEM and X-ray scattering can be used to obtain complementary and consistent size information for nanometer-scale gold particles that mimic ionic aggregates.<sup>16</sup> In that study, it was shown that thinner HAADF-STEM specimens improve the signal-to-noise ratio in images, reduce beam damage, and enable imaging at higher magnifications by reducing the number of inelastic scattering events. Here, we apply this improved HAADF-STEM method along with X-ray scattering to study the morphology of an amorphous poly(styrene-*ran*-methacrylic acid) (SMAA) ionomer neutralized with copper. The results provide the first report of quantitative agreement regarding the *size of spherical ionic aggregates* as determined from both real-space morphological data, as measured directly by STEM, and reciprocal-space scattering data interpreted using the Yarusso–Cooper model.

**Results and Discussion.** A SMAA copolymer was solution neutralized,<sup>17</sup> and the Cu-neutralized SMAA ionomer product was isolated by room-temperature solvent casting (12 h) and dried under vacuum.<sup>18</sup> The intensity of scattered X-rays as a function of scattering vector ( $q$ ) shows three isotropic peaks within  $q = 1.6$ – $16$  nm<sup>-1</sup>, Figure 1.<sup>19</sup> The “ionomer” peak at  $\sim 3.7$  nm<sup>-1</sup> confirms the presence of ionic aggregates and is absent from the scattering pattern of the un-neutralized acid copolymer. The peaks at  $\sim 7$  and  $\sim 13$  nm<sup>-1</sup>, commonly referred

\* To whom correspondence should be addressed. E-mail: winey@seas.upenn.edu.

<sup>†</sup> Department of Physics and Astronomy.

**Table 1. Fitting Parameters Obtained from Empirical Scattering Model for a Cu-Neutralized SMAA Ionomer**

functions and their fitting parameters	best-fit value
Yarusso–Cooper $I_{YC}(q)$	
aggregate radius ( $R_1$ )	$0.50 \pm 0.01$ nm
radius of closest approach ( $R_{CA}$ )	$0.71 \pm 0.01$ nm
average sample volume per aggregate ( $V_p$ )	$4.2 \pm 0.5$ nm <sup>3</sup>
peak amplitude ( $A$ )	$89 \pm 3$ a.u.
Lorentzian $L_1(q)$	
peak amplitude ( $A_{L_1}$ )	$52 \pm 1$ a.u.
peak position ( $q'_1$ )	$7.1$ nm <sup>-1</sup>
half width at half-maximum ( $\kappa_1$ )	$1.6 \pm 0.01$ nm <sup>-1</sup>
Lorentzian $L_2(q)$	
peak amplitude ( $A_{L_2}$ )	$202 \pm 1$ a.u.
peak position ( $q'_2$ )	$13.2$ nm <sup>-1</sup>
half width at half-maximum ( $\kappa_2$ )	$1.9 \pm 0.01$ nm <sup>-1</sup>
Additive constant, $C$	$130 \pm 1$ a.u.

to as the “polymerization” and “amorphous” PS peaks, respectively, are typical of amorphous polystyrene and are present in the scattering patterns of both un-neutralized SMAA copolymer and PS homopolymer.<sup>20–22</sup>

The scattering data across this angular range were modeled using the summation of three functions and a constant. The “ionomer” scattering peak was fit with the Yarusso–Cooper model, the development of which is reported elsewhere:<sup>5</sup>

$$I_{YC}(q) = A \cdot \Phi^2(qR_1) \frac{1}{1 + (8V_{CA}/V_p)\epsilon \cdot \Phi(2qR_{CA})} \quad (1)$$

where

$$\Phi(x) = 3 \frac{\sin(x) - x \cos(x)}{x^3}$$

There are four independent fitting parameters: the ionic aggregate radius  $R_1$ , the radius of closest approach  $R_{CA}$  that limits the spatial correlation between two aggregates, the average sample volume per aggregate  $V_p$ , and the peak amplitude  $A$ , which incorporates all of the factors affecting the absolute value of intensity. Note that, as implemented, our model assumes a single ionic aggregate radius with no polydispersity. The polymerization and amorphous scattering peaks were each fit with a Lorentzian function:

$$L(q) = \frac{A_L \cdot \kappa^2}{(q - q')^2 + \kappa^2} \quad (2)$$

where  $A_L$  is the peak amplitude,  $q'$  is the peak position, and  $\kappa$  is the half width at half-maximum. In addition to the three fitting functions, an additive constant ( $C$ ) was included to account for instrumental background scattering. Thus, our empirical functional form for the SAXS data, which includes the Yarusso–Cooper structural model and terms to describe both sample-derived and instrumental background, is given by:

$$I(q) = I_{YC}(q) + L_1(q) + L_2(q) + C \quad (3)$$

While previous applications of the Yarusso–Cooper model fit only the “ionomer” peak, fitting with this empirical model accounts more rigorously for the contributions of the PS features to the adjacent “ionomer” peak. A least-squares regression<sup>23</sup> optimized the independent fitting parameters and generated the best-fit curve, which is shown in comparison with the scattering data (Figure 1). The individual functions used to generate this best-fit curve are also shown and illus-

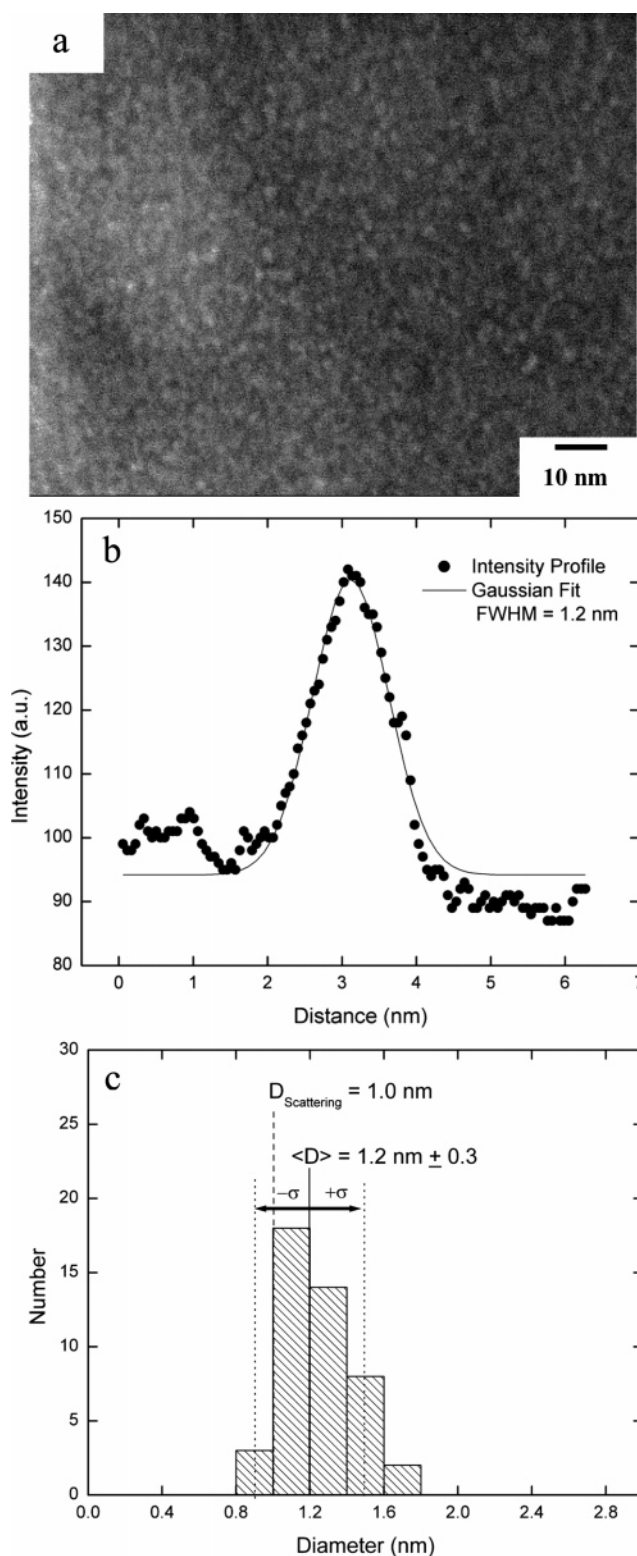


**Figure 2.** (a) HAADF STEM image of Cu-SMAA shows a dense, uniform distribution of spherical Cu-rich ionic aggregates. (b) A representative STEM intensity profile as scanned across an ionic aggregate in which each point corresponds to the pixel intensity. The best-fit Gaussian curve to this intensity profile has a fwhm of 1.2 nm. (c) Size distribution histogram illustrating the mean ionic aggregate diameter as measured by STEM ( $\langle D_{STEM} \rangle$ ) along with the standard deviation ( $\sigma$ ). For comparison, the diameter of the ionic aggregates obtained by X-ray scattering from the same sample is included.

trate the importance of peak overlap. The  $\chi$ -squared parameter (a measure of how well a model fits scattering data) is less than 2, indicating good agreement between the data and our

model. The fitting parameters for each function are reported along with the statistical uncertainty associated with each fitting parameter in Table 1. (These uncertainties also account for correlations between parameters.) The fitting parameters of the Yarusso–Cooper model ( $R_1$ ,  $R_{CA}$ ,  $V_p$ ) are consistent with previous reports of similar amorphous ionomers.<sup>5,9</sup> Our scattering results interpreted with our empirical model indicate the presence of a uniform distribution of monodisperse, spherical ionic aggregates with a diameter of 1.0 nm.

Using HAADF-STEM, we have imaged these nanoscale ionic aggregates in thin specimens sectioned from the same bulk Cu–SMAA ionomers characterized by X-ray scattering.<sup>24,25</sup> The bright spots visible in the image of Figure 2a correspond to areas of higher average atomic number (i.e., Cu-rich aggregates) within a matrix of lower average atomic number. The Cu-rich aggregates appear to be spherical, monodisperse, and distributed uniformly throughout the specimen. The sizes of the ionic aggregates were determined by fitting the intensity profiles across the ionic aggregates with Gaussian curves.<sup>16</sup> Figure 2b shows a representative line intensity profile of a Cu-rich ionic aggregate fit with a Gaussian curve having a fwhm = 1.2 nm. Using this method on >40 ionic aggregates, we have determined an average diameter of  $1.2 \pm 0.3$  nm, where the error is the standard deviation of these measurements, Figure 2c. This standard deviation corresponds to a measurement uncertainty of <2 pixels per ionic aggregate. Thus, our results are consistent with a monodisperse size distribution of ionic aggregates convoluted with finite instrumental resolution.

Figure 2c also presents both the mean diameter measured from STEM ( $\langle D_{\text{STEM}} \rangle$ ) and the best-fit parameter from the X-ray scattering data ( $D_{\text{Scattering}}$ ). For this particular ionomer sample, the real-space, model-independent ionic aggregate size determined by STEM and the size determined by X-ray scattering data interpreted by the Yarusso–Cooper model are consistent. Both imaging and scattering data indicate uniformly distributed, relatively monodisperse, spherical ionic aggregates with diameters of ~1.0 nm. This is the first report of quantitatively consistent data from X-ray scattering methods and STEM imaging methods regarding the *size of ionic aggregates*.

Our goal is to rigorously advance the study of ionomer morphology and to correlate morphologies with macroscopic properties such as toughness and ion transport. Combining direct imaging and X-ray scattering will provide a comprehensive view of how changes in structure and processing affect the fundamental interactions of ionomers. A robust and reliable scattering model is required to facilitate such studies. This communication provides validation of the Yarusso–Cooper ionomer scattering model with two important caveats. First, previous STEM investigations of ionomers suggest a variety of ionomer morphologies depending on copolymer type, counterion type, and processing methods. Thus, future studies must determine the domain over which the Yarusso–Cooper model describes the size of the ionic aggregates within SMAA ionomers (as a function of processing methods, counterion type, level of neutralization, acid content, etc.) and subsequently for other ionomer materials. Second, it remains to reconcile other aspects of the Yarusso–Cooper scattering model, namely the average sample volume per ionic aggregate, using both scattering and STEM data. Work to address both of these caveats is currently underway.

**Acknowledgment.** Funding was provided by the National Science Foundation (DMR02-35106 and DMR05-20020). We acknowledge Prof. Joon-Seop Kim of Chosun University for providing SMAA copolymers and Dr. Doug Yates of the PENN Regional Nanotechnology Facility for helpful discussions and technical assistance. Nicholas M. Benetatos acknowledges funding provided through an Augustus T. Ashton fellowship at the University of Pennsylvania.

## References and Notes

- (1) Eisenberg, A.; Kim, J.-S. *Introduction to Ionomers*; John Wiley & Sons: New York, 1998.
- (2) Marx, C. L.; Caulfield, D. L.; Cooper, S. L. *Macromolecules* **1973**, *6*, 344–353.
- (3) MacKnight, W. J.; Taggart, W. P.; Stein, R. S. *J. Polym. Sci., Polym. Symp.* **1974**, *45*, 113–128.
- (4) Roche, E. J.; Stein, R. S.; Russell, T. P.; MacKnight, W. J. *J. Polym. Sci., Polym. Phys. Ed.* **1980**, *18*, 1497–1512.
- (5) Yarusso, D.; Cooper, S. L. *Macromolecules* **1983**, *16*, 1871–1880.
- (6) Fournet, G. *Acta Crystallogr.* **1951**, *4*, 293–301.
- (7) Ding, Y. S.; Hubbard, S. R.; Hodgson, K. O.; Register, R. A.; Cooper, S. L. *Macromolecules* **1988**, *21*, 1698–1703.
- (8) Kinning, D. J.; Thomas, E. L. *Macromolecules* **1984**, *17*, 1712–1718.
- (9) Yarusso, D.; Cooper, S. L. *Polymer* **1985**, *26*, 371–378.
- (10) Laurer, J.; Winey, K. I. *Macromolecules* **1998**, *31*, 9106–9108.
- (11) Winey, K. I.; Laurer, J. H.; Kirkmeyer, B. P. *Macromolecules* **2000**, *33*, 507–513.
- (12) Kirkmeyer, B. P.; Weiss, R. A.; Winey, K. I. *J. Polym. Sci., Part B: Polym. Phys.* **2001**, *39*, 477–483.
- (13) Kirkmeyer, B. P.; Taubert, A.; Kim, J.-S.; Winey, K. I. *Macromolecules* **2002**, *35*, 2648–2653.
- (14) Taubert, A.; Winey, K. I. *Macromolecules* **2002**, *35*, 7419–7426.
- (15) Benetatos, N. M.; Winey, K. I. *J. Polym. Sci., Part B: Polym. Phys.* **2005**, *43*, 3549–3554.
- (16) Benetatos, N. M.; Smith, B. W.; Heiney, P. A.; Winey, K. I. *Macromolecules* **2005**, *38*, 9251–9257.
- (17) A small quantity of copper(II) acetate monohydrate (Aldrich, fw 199.65) was dehydrated by heating under vacuum at ~90–100 °C for 12 h. The dehydrated copper(II) acetate salt (28 mg, 0.171 mmol) was dissolved in methanol and added dropwise to a gently refluxing solution of poly(styrene-*ran*-methacrylic acid) (SMAA) (6.2 mol % MAA) in toluene. The addition of the copper acetate solution was performed over a period of ~30 min, and the resulting mixture was stirred for 12 h at ~100 °C. The final solvent ratio was 90/10 toluene/methanol by volume.
- (18) Materials were dried under vacuum at ~90 °C for 12 h and stored under anhydrous conditions.
- (19) The SAXS apparatus consisted of a Nonius FR591 rotating-anode generator operated at 40 kV  $\times$  85 mA, mirror-monochromator focusing optics, an evacuated flight path, and a Bruker HiSTAR multiwire two-dimensional detector. Data were acquired over 1 h intervals at a sample–detector distance of 11 cm. Two-dimensional data reduction, analysis, and curve fitting were performed using Datasqueeze software.
- (20) Wecker, S. M.; Davidson, T.; Cohen, J. B. *J. Mater. Sci.* **1972**, *7*, 1249–1259.
- (21) Mitchell, G. R.; Windle, A. H. *Polymer* **1984**, *25*, 906–920.
- (22) Ayyagari, C.; Bedrov, D.; Smith, G. D. *Macromolecules* **2000**, *33*, 6194–6199.
- (23) Heiney, P. A. *Commun. Powder Diffr. Newsl.* **2005**, *32*, 9–11.
- (24) STEM experiments were performed on a JEOL 2010F field emission electron microscope operated at 197 kV with a 70  $\mu$ m condenser aperture. Images were acquired using a high-angle annular dark-field (HAADF) scintillating detector with linear intensity response.
- (25) STEM specimens were sectioned at room temperature with a cutting speed of 0.2 mm/s using a Reichert–Jung ultramicrotome equipped with a diamond knife. Nominal section thickness was 30 nm.

MA0608976